

# Fabrication of porous bioceramics with porosity gradients similar to the bimodal structure of cortical and cancellous bone

Y. H. Hsu · I. G. Turner · A. W. Miles

Received: 30 June 2006 / Accepted: 21 July 2006 / Published online: 12 June 2007  
© Springer Science+Business Media, LLC 2007

**Abstract** The aim of this study was to fabricate porous implant materials with graded pore structures similar to the bimodal structure of cortical and cancellous bone. Porous hydroxyapatite/tricalcium phosphate (HA/TCP) bioceramics with interconnected porosity and controlled pore sizes required to simulate natural bone tissue morphology were fabricated by a novel technique of vacuum impregnation of reticulated polymeric foams with ceramic slip. Functionally gradient materials (FGMs) with porosity gradients were made by joining different pore per inch (ppi) foams together by either stitching or pressfitting to form templates. Post production, no defects could be seen at the interface between the two different porosity sections. The macropore sizes of the HA/TCP bioceramics were larger than 100  $\mu\text{m}$  which is appropriate for bone ingrowth. A sample with a graded porous structure which is close to the human bone morphology was also developed. The two component structures were conspicuously different but joined together firmly. Four point bend testing of FGM samples showed them to have similar mechanical properties to homogeneous ceramics based on foam templates with uniform pore sizes, with no evidence of interfacial weakness. Many potential biomedical applications could be developed utilising graded porous structures. The ease of processing will make it possible to fabricate a range of complex shapes for different applications.

## Introduction

Bone grafts are necessary in orthopaedic surgery for filling bone cavities, treatment of nonunion and replacement of bone lost during trauma and tumour removal. Porous calcium phosphate based ceramics are attractive for use as synthetic bone grafts allowing successful tissue ingrowth, which further enhances the implant-tissue attachment [1–6]. The degree of interconnectivity and the nominal pore size are critical factors that determine the success of the implants. It is generally accepted that a minimum pore size of 100  $\mu\text{m}$  is necessary for the porous implant materials to function well and a pore size greater than 200  $\mu\text{m}$  is an essential requirement for osteoconduction. However, research has suggested that the degree of interconnectivity is more critical than the pore size [7, 8].

Functional gradient materials (FGMs) are defined as materials which have a gradient of properties (microstructure and/or composition) which change with position [9, 10]. In recent times, FGMs have been developed for use in engineering fields. The materials exhibiting graded or layered porous structures are a special case of functionally graded materials and are interesting for several applications. FGMs have also attracted much attention in the field of biomaterials [11–17]. Bone has a functionally graded structure from the surface of cortical bone towards the inner cancellous bone. Therefore, the design of porous implant materials with a porosity gradient mimicking as closely as possible the bimodal structure of bone (compact and spongy) and with a sufficient degree of interconnectivity is the most important challenge [14, 18].

Tampieri et al. [14] produced porous HA with a porosity gradient in order to simulate bone tissue morphology. The sample produced had a high-porosity portion (representing spongy bone) which allowed good and fast bone ingrowth and

Y. H. Hsu · I. G. Turner (✉) · A. W. Miles  
Centre for Orthopaedic Biomechanics, Department of  
Mechanical Engineering, University of Bath, Claverton Down,  
Bath BA2 7AY, UK  
e-mail: I.G.Turner@bath.ac.uk

a low-porosity side (similar to compact bone) which could withstand early physiologic mechanical stress [14]. Cylindrical specimens exhibiting a porosity gradient showed promising behaviour after implantation in the femurs of rabbits. Newly formed bone grew in direct contact with the ceramic in a very short time [14]. Arita et al. [13] used a tape casting method to produce a thin hydroxyapatite layer 150–200  $\mu\text{m}$  thick and the HA layer obtained allowed them to produce laminates with desired porosity gradients, up to several millimetres thick but the pore size was limited to only several micrometres which might be inadequate for bone ingrowth. Vaz et al. [11] used a multiple slip-casting technique, in order to obtain dual-layer samples with different sized porosities. It was proposed that the external layer, because of its porosity (40%), controlled by the addition of organic compounds (PVC), should promote bone ingrowth. It was also proposed that the internal denser layer (porosity: 10%), due to the addition of lithium phosphate ( $\text{Li}_3\text{PO}_4$ ) as sintering additive, should give mechanical resistance to the implant. Werner et al. [12] developed functionally pore-graded materials with the aim of improving the mechanical strength of hydroxyapatite (HA) ceramics used as bone implants and to enhance cellular penetration. The macropores in the outer layers would provide access for cell, blood vessels and enhance new bone formation whereas the inner dense ceramic structure improved the mechanical stability of the implants. The results showed that the bending strength of the pore-graded ceramics was approximately 50% higher compared to HA of the same pore volume fraction but without the gradient structure. The bending strength for the pore-graded structure was in the range of 6–9 MPa and one single pore size sample was in the range of 4–5 MPa. Similar work was carried out by Carotenuto et al. [19], who made dense/porous hydroxyapatite laminates by slip casting technology. Their results showed the first layer consisted of macroporous hydroxyapatite with high osteoconductive properties and the second layer was a dense hydroxyapatite substrate able to provide the laminate with good mechanical properties.

Although a large number of papers have reported on fabrication of pore gradient bioceramics, many of them have layer fractures and nearly all of them can only be used to manufacture simple shapes with flat layered porous gradient structures which are not representative of the normally circular cross section of long bone.

## Experimental procedure

### Fabrication techniques for functional gradient materials (FGMs)

Two grades of calcium phosphate powder, TCP 118 and TCP 130 (Thermphos), were used in this study. Varying the

blend ratios of TCP 118 and TCP 130 and sintering temperature changed the ratios of HA and TCP in the sintered samples. In this study, TCP 118 and TCP 130 powders (1:1) were gradually added to distilled water to prepare slips of 1,000 g of powder per litre (100 wt%).

The organic foams, which were completely burned out during sintering were made of polyurethane (PU) which had one of three porosities: 20 pores per inch (ppi), 30 ppi and 45 ppi (Sydney Heath and Sons Ltd.). In order to make a FGM with porosity gradients similar to the bimodal structure of cortical and cancellous bone, two different foams were joined together either by stitching or pressfitting. Figure 1 shows two foams which were joined by stitching. A hot cut method was applied to make cylindrical foam templates by using stainless steel cylinders of different dimensions as shown in Fig. 2. Figure 3 shows a cylindrical foam and a hollow foam produced by the hot cut method and Fig. 4 shows these two foams joined together by pressfitting. Foams with different ppi could be used as the cylindrical foams and the hollow foams. The relative ratio of the diameter of the insert foam and the diameter of the hole can be changed.

The foams were substantially impregnated with ceramic slip by a vacuum impregnation method as described in earlier published work [20]. The dried green samples were sintered in a programmable furnace at 1,280  $^{\circ}\text{C}$ . The final composition of the sintered samples was 75% HA and 25% TCP.

In order to obtain samples with graded pore structures the following approach was employed. A method of dipping foams into a slip of lower viscosity (less than 6,000 cps) was used to make a porous HA/TCP with higher porosity as illustrated in Fig. 5(a). A low porosity green state sample from the vacuum impregnation (Fig. 5(b)) and the high porosity green state samples, obtained as in (Fig. 5(a)), could also be combined together by pressfitting as shown in Fig. 5(c). In this way, it was possible to make a FGM with a much greater porosity gradient. The relative

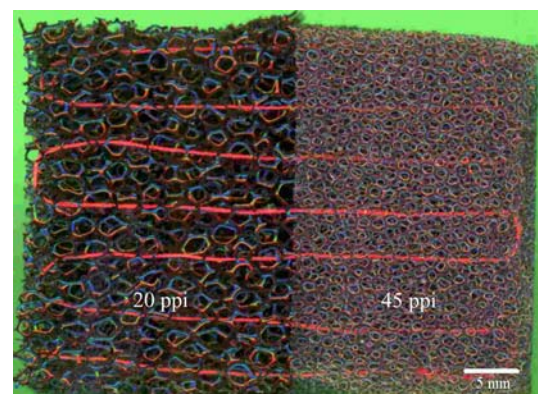


**Fig. 1** Two different ppi foams joined together by stitching



**Fig. 2** Stainless steels cylinders used in the hot cutting method

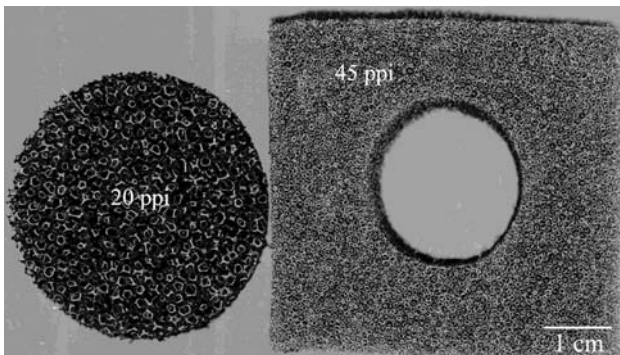


**Fig. 3** Foams geometries produced using the hot cutting method

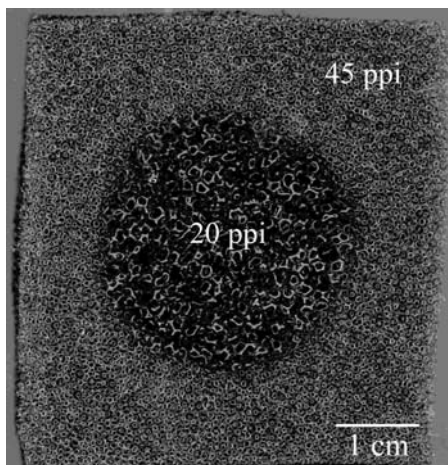


**Fig. 4** Two different ppi foams joined together by pressfitting

ratio of the diameter of the insert foam and the diameter of the hole can be changed.

**Fabrication of four-point bend test samples**

In order to estimate the strength of the interface between the two different structures making up the FGM, four-point bend testing was employed. The FGM was produced by

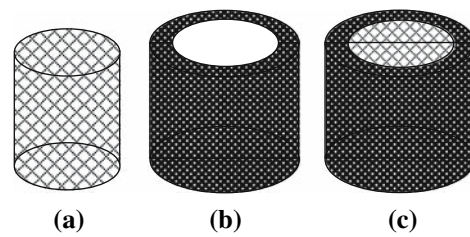


**Fig. 5** An illustration of the method to obtain samples with two extremely different graded pore structures as close as possible to human bone morphology (a) high porosity sample from dipping method (b) low porosity sample from vacuum impregnation method (c) sample (a) and (b) joined together by pressfitting

joining 20 and 45 ppi foams together by stitching as shown in Fig. 6, to make a large block of material 70 mm × 70 mm × 25 mm. Homogeneous porous HA/TCP bioceramics from 20, 30 and 45 ppi foams were produced for comparative purposes.

The large sintered blocks of FGM and homogeneous porous HA/TCP bioceramic were sectioned into rectangular bars with dimensions of 45 mm × 5 mm × 4 mm. The rectangular bars obtained from the FGM block contained two different porous structures in one bar. Rough and chipped edges were ground off with silicon carbide paper. The aim of the testing was to compare the strength of the FGM and homogeneous materials and to investigate if the interface of the FGM was a source of weakness. Up to eight samples made from each ppi foam were tested to obtain average values for the four-point bend strength. The samples were tested using an Instron 1122 testing machine with a crosshead speed of 0.5 mm/min and the span was 20 mm × 40 mm. Four-point bend testing was used rather than three-point bending. Three-point bend testing has limitations in that the maximum flexural stress is at the

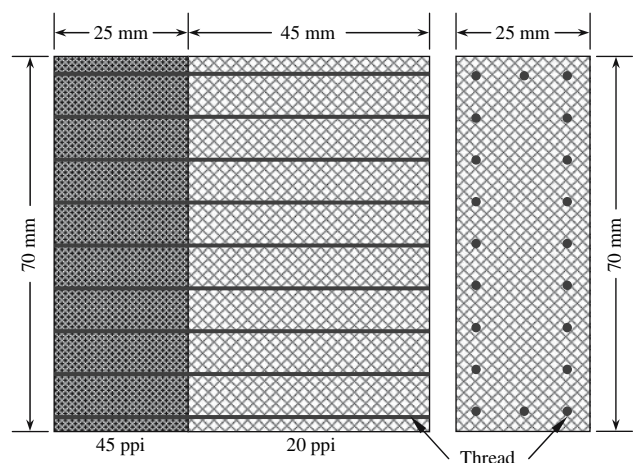


**Fig. 6** Schematic representation of the stitching method used to join two foams together

point of load application but linearly decreases to zero at the outer supports. The sample will tend to fail near the point of load application. In four-point bending, there is a large region of maximum flexural stress between the inner supports so this test should be able to explore the source of weakness more accurately.

The four-point bend strengths ( $\sigma$ ) were calculated using the equation:

$$\sigma \text{ (Pa)} = 3F(L - L_1)/2bd^2 \text{ (N/m}^2\text{)}$$

where  $F$  is the applied force,  $L$  the span of the support roller,  $L_1$  the separation of the loading span,  $b$  the sample width, and  $d$  is the sample thickness.

## Results and discussion

### Functional gradient materials (FGMs)

Figure 7 shows the external and internal appearance of samples generated from a template that consisted of sections of 20 ppi and 45 ppi foams joined together by stitching. This technique demonstrated that porous HA/TCP with two or more different levels of porosity could be produced in a single block. Figure 8 shows the samples of 20 ppi and 45 ppi foams joined by pressfitting. Foams with

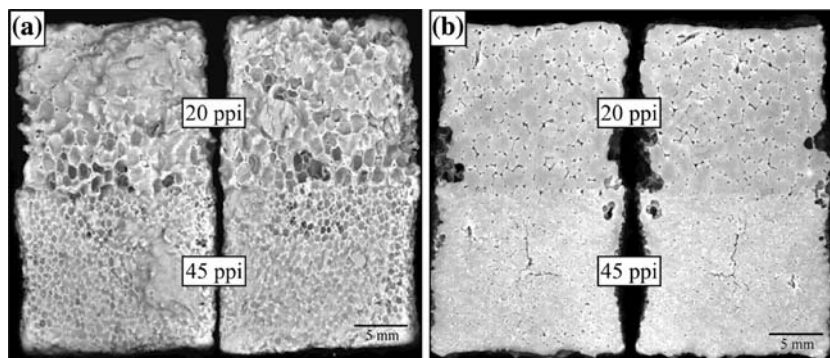
different porosities (20, 30, 45 ppi) could be utilized as the centre or hollow foam according to the desired application.

Figure 9 is an SEM micrograph of the interface of the sample which contains two different porous structures. No defects could be seen at the interface between the two different foam structures. Using this method to make a FGM ensured that the pores present in different parts of the composite structure were interconnected. The polymer foams were joined by stitching or pressfitted together, consequently, the interface of the two foams had a number of definite points of contact. These converted to interconnected channels in the resultant ceramic blocks. A sample with a graded porous structure which is much closer to the human bone morphology is shown in Fig. 10. The outside denser structure was made by vacuum impregnation and inside, the more porous structure, was made by a dipping method. These two structures were conspicuously different but joined together firmly.

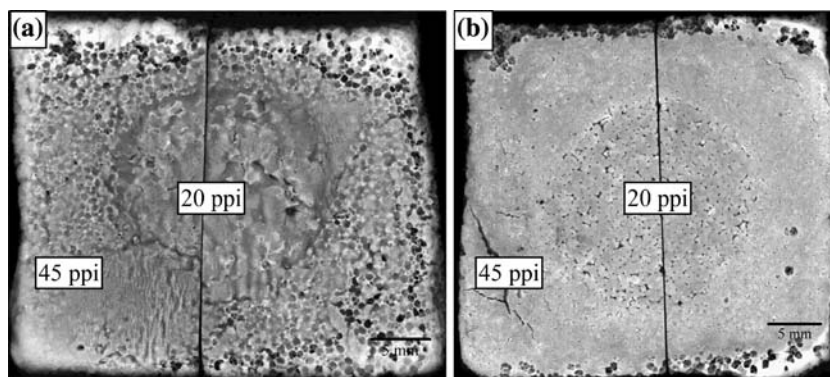
### Four-point bend testing

In order to compare the strengths of the FGM and homogeneous materials and to investigate if the interface of the FGM was a source of weakness, four-point bend testing was employed. The FGM samples were tested with a crosshead speed of 0.5 mm/min and the span was 20 mm  $\times$  40 mm. Figure 11 shows rectangular bars with

**Fig. 7** (a) The external appearance and (b) a transverse section of the HA/TCP with the combination two different pores sizes



**Fig. 8** (a) The external appearance and (b) transverse sections of the HA/TCP with the combination two different pore sizes



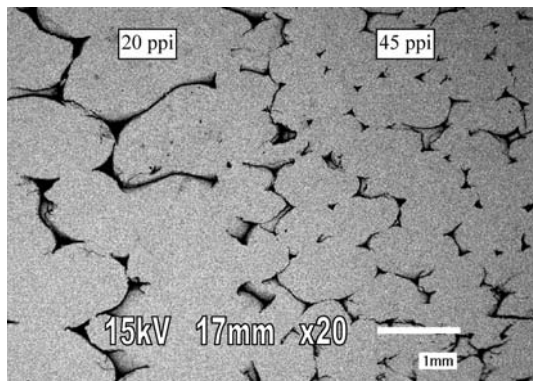


**Fig. 9** Micrograph of the interface of the sample which consisted of 20 and 45 ppi foams

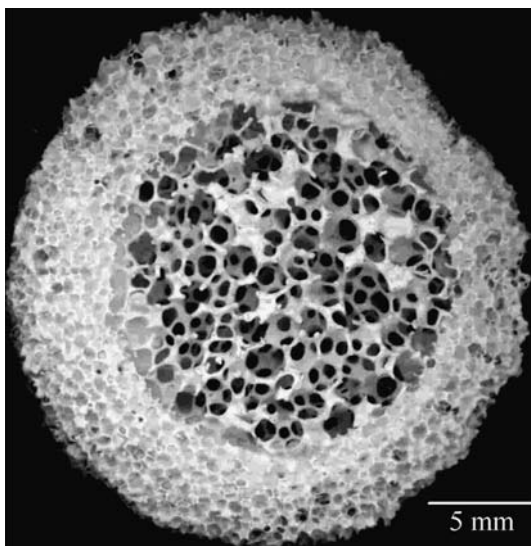


**Fig. 10** The external appearance of a sample produced by joining two porous structures made by vacuum impregnation and dipping

dimensions of 45 mm × 5 mm × 4 mm comprising two different porosity structures. The interface of the two structures was within the upper span which meant that it sustained the highest loading. Figure 12 shows the bars after four-point bend testing. The interface of the FGM was not a source of weakness as the fracture did not occur at interface. Figure 13 and Table 1 show the four-point bend strengths of porous HA/TCP bioceramics resulting from 20, 30 and 45 ppi foams with 100 wt% solid loading slip and FGM samples. The average four-point bending strength of the homogeneous porous samples made from various ppi foams was in the range of 18.32–19.65 MPa and that for the FGM was 15.61 ± 2.72 MPa. FGM had the lowest average four-point bend strength. Table 2 shows the Student *T*-test results for the strengths of porous HA/TCP bioceramics from various ppi foams and FGM samples. It can be seen that there was no difference between the FGM

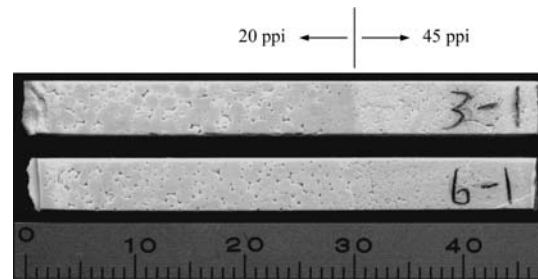


**Fig. 11** Bars of FGM sectioned from a large block for four-point bend testing

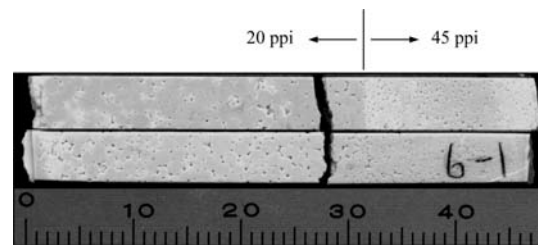


**Fig. 12** The fracture mode of the FGM bars after four-point bend testing

and samples made using the 20 and 30 ppi foams but the FGM had probably lower strength than that in the sample made from 45 ppi foam. The lower strength of FGM might result from an insufficient compression step during impregnation as intense compression may damage the structure of stitching. A longer vacuum period might improve the impregnation and result in an increase in the strength of the FGM. However, the fracture of the FGM was in the area made from 20 ppi foam which had a lower strength than that based on the 45 ppi foam template. The strength of FGM was comparable to that of the sample made from 20 ppi foam. This confirmed that the four-point bend strengths of the FGM made by this method were similar to the homogeneous porous sample and the interface was not a source of weakness.

## Conclusions

Novel techniques have been developed for the manufacture of functional gradient materials. It has been demonstrated that FGM with two different pore sizes with no fractures at the interface can be fabricated successfully. The average four-point bend strength of the FGM was comparable to that for the homogeneous porous samples. The interface of the FGM was not a source of weakness. Using this method to make a FGM ensured that the pores present in different parts of the composite structure were interconnected.

**Fig. 13** The four-point bending strength of FGM samples compared to that for homogeneous porous HA/TCP bioceramics from various ppi foams

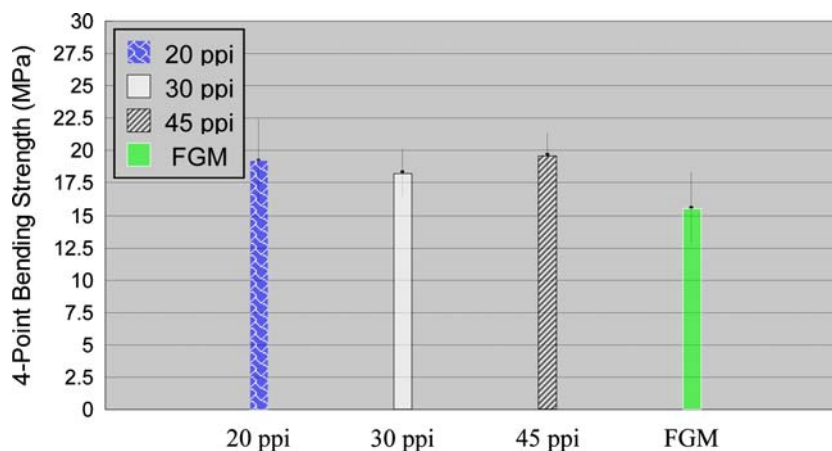


**Table 1** The four-point bend strengths of homogeneous porous HA/TCP bioceramics from different ppi foams and FGM samples

Four-point bend strength (MPa)			
20 ppi	30 ppi	45 ppi	FGM
19.20 ± 3.22	18.32 ± 1.81	19.65 ± 1.75	15.61 ± 2.72

**Table 2** Student *T*-test results for the four-point bend strengths of homogeneous porous HA/TCP bioceramics from various ppi foams and FGM samples

Foam (ppi)	20	30	45	FGM
20		O	O	O
30	O		O	O
45	O	O		#
FGM	O	O	#	

#, Probable difference; O, Difference not established

The technique developed is efficient and reproducible. Integrity and continuity across the interface indicate the enormous potential to produce complex shapes when compared to most existing methods which can only be used to manufacture flat layered porous graded structures.

Simulation of a bimodal structure closer to that found in natural bone is possible. Many potential biomedical applications could be developed utilising graded porous structures. The ease of processing will make it possible to fabricate a range of complex shape for different applications.

**Acknowledgements** The authors would like to thank the University of Bath and Stryker Howmedica Osteonics for their support.

## References

1. A. TAMPIERI, G. CELOTTI, S. SPRIO, A. DELCEGLIANO and S. FRANZESE, *Biomaterials* **22** (2001) 1365
2. T. M. G. CHU, D. G. ORTON, S. J. HOLLISTER, S. E. FEINBERG and J. W. HALLORAN, *Biomaterials* **23** (2002) 1283
3. J. TIAN and J. TIAN, *J. Mater. Sci.* **36** (2001) 3061
4. D. J. A. NETZ, P. SEPULVEDA, V. C. PANDOLFELLI, A. C. C. SPADARO, J. B. ALENCASTRE, M. V. L. B. BENTLEY and J. M. MARCHETTI, *Int. J. Pharm.* **213** (2001) 117
5. B. FLAUTRE, M. DESCAMPS, C. DELECOURT, M. C. BLARY and P. HARDOUIN, *J. Mater. Sci. Mater. Med.* **12** (2001) 679
6. J. X. LU, B. FLAUTRE, K. ANSELME and P. HARDOUIN, *J. Mater. Sci. Mater. Med.* **10** (1999) 111
7. J. H. KUHNE, R. BARTL, B. FRISH, C. HANMER, V. JANSOON and M. ZIMMER, *Acta Orthop. Scand.* **65** (1994) 246
8. P. S. EGGLI, W. MULLER and R. K. SCHENK, *Clin. Orthop. Relat. Res.* **232** (1988) 127
9. A. MORTENSEN and S. SURESH, *Int. Mater. Rev.* **40** (1995) 239
10. B. KIEBACK, A. NEUBRAND and H. RIEDEL, *Mater. Sci. Eng.* **A362** (2003) 81
11. L. VAZ, A. B. LOPES and M. ALMEIDA, *J. Mater. Sci. Mater. Med.* **10** (1999) 239
12. J. WERNER, B. LINNEN-KRCMAR, W. FRIESS and P. GREIL, *Biomaterials* **23** (2002) 4285
13. I. H. ARITA, V. M. CASTANO and D. S. WILKINSON, *J. Mater. Sci. Mater. Med.* **6** (1995) 19
14. A. TAMPIERI, G. CELOTTI, S. SPRIO, A. DELCEGLIANO and S. FRANZESE, *Biomaterials* **22** (2001) 1365
15. E. RONCARI and C. GALASSI, *J. Mater. Sci. Lett.* **19** (2000) 33
16. W. POMPE, H. WORCH, M. EPPLE, W. FRIESS, M. GELINSKY, P. GREIL, U. HEMPEL, D. SCHARNWEBER and K. SCHULTE, *Mater. Sci. Eng.* **A362** (2003) 40
17. M. WANG, X. Y. YANG, K. A. KHOR and Y. WANG, *J. Mater. Sci. Mater. Med.* **10** (1999) 269
18. K. A. HING, S. M. BEST and W. BONFIELD, *J. Mater. Sci. Mater. Med.* **10** (1999) 135
19. G. CAROTENUTO, G. SPAGNUOLO, L. AMBROSIO and L. NICOLAIS, *J. Mater. Sci. Mater. Med.* **10** (1999) 671
20. Y. H. HSU, I. G. TURNER and A. W. MILES, *Key Eng. Mater.* **284–286** (2005) 305